J Biomol NMR (2011) 49:9–15
DOI 10.1007/s10858-010-9461-5

COMMUNICATION

Recovering lost magnetization: polarization enhancement in biomolecular NMR

Adrien Favier · Bernhard Brutscher

Received: 8 October 2010 / Accepted: 26 November 2010 / Published online: 30 December 2010

Abstract Experimental sensitivity remains a major drawback for the application of NMR spectroscopy to fragile and low concentrated biomolecular samples. Here we describe an efficient polarization enhancement mechanism in longitudinal-relaxation enhanced fast-pulsing triple-resonance experiments. By recovering undetectable ^{1}H polarization originating from longitudinal relaxation during the pulse sequence, the steady-state ^{15}N polarization becomes enhanced by up to a factor of ~ 5 with respect to thermal equilibrium yielding significant sensitivity improvements compared to conventional schemes. The benefits of BEST-TROSY experiments at high magnetic field strength are illustrated for various protein applications, but they will be equally useful for other protonated macromolecular systems.

Keywords BEST · Fast NMR · Longitudinal-relaxation enhancement · Protein · Sensitivity · TROSY

Electronic supplementary material The online version of this article (doi:10.1007/s10858-010-9461-5) contains supplementary material, which is available to authorized users.

A. Favier · B. Brutscher (✉)
IBS, Institut de Biologie Structurale Jean-Pierre Ebel,
41 rue Jules Horowitz, 38027 Grenoble, France
e-mail: bernhard.brutscher@ibs.fr

A. Favier · B. Brutscher
CEA, Grenoble, France

A. Favier · B. Brutscher
CNRS, Grenoble, France

A. Favier · B. Brutscher
Université Joseph Fourier, Grenoble, France

An important drawback of biomolecular NMR spectroscopy remains its intrinsically low sensitivity. Therefore many efforts are made for the development of new NMR hardware, e.g. high magnetic fields, cryogenically-cooled probes, or dynamic nuclear polarization that increase the intrinsic sensitivity. A complementary and less expensive way of improving experimental sensitivity is the development of advanced NMR pulse sequences that are optimized in terms of coherence-transfer pathways to achieve the highest possible signal to noise (S/N) ratio for a given experimental setup. Herein we show how signal that is lost by spin-relaxation during the experiment can be recovered, to a large extent, using recently introduced BEST-TROSY techniques (Farjon et al. 2009; Lescop et al. 2010). BEST-TROSY contains a built-in module for the conversion of undetected ^{1}H polarization into enhanced ^{15}N polarization. As shown here, this polarization-enhancement technique yields improved sensitivity in a variety of NMR experiments that are commonly used for the study of proteins and nucleic acids.

The sensitivity of an NMR experiment is directly proportional to the equilibrium or, in multi-scan experiments, the steady-state spin polarization available at the beginning of the pulse sequence. Polarization enhancement methods thus provide valuable tools to increase the sensitivity of an NMR experiment. Steady-state polarization enhancement is achieved by increasing the magnetic field strength, by transferring polarization from high-γ to low-γ spins, or by accelerating the longitudinal relaxation of the excited nuclear spins. The latter approach is exploited in longitudinal-relaxation optimized sequences (Pervushin et al. 2002) such as the SOFAST (Schanda and Brutscher 2005; Schanda et al. 2005) and BEST family (Lescop et al. 2007; Schanda et al. 2006) of experiments. In a few rare cases, the steady-state polarizations of two distinct nuclear species can be merged into one observable NMR signal for higher

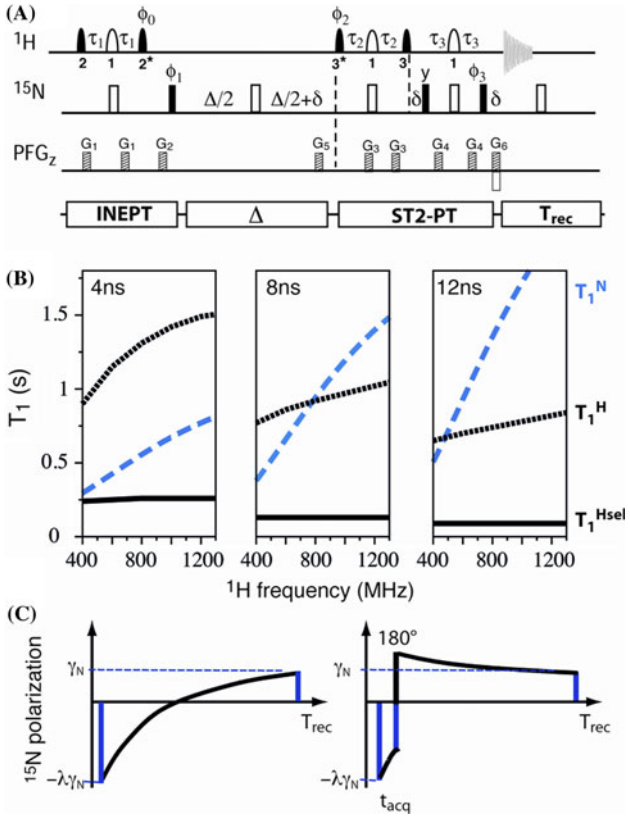

◀**Fig. 1** **a** Gradient-selected BEST-TROSY pulse sequence. Chemical shift and scalar coupling evolution during the ^{15}N relaxation delay Δ is refocused by a 180° ^{15}N pulse. This sequence has been used for the experimental data shown in Fig. 2c and d. For real NMR experiments the relaxation delay Δ is replaced by either a frequency editing delay (t_1) or further coherence transfer periods. *Filled and open symbols* correspond to 90° and 180° rf pulses, respectively. Amide ^{1}H pulses typically cover a bandwidth of 4 ppm (centered at 8.5 ppm), and have the following shapes and durations at 800 MHz: (1) REBURP (Geen and Freeman 1991), 1.5 ms (δ_1), (2) PC9 (Kupce and Freeman 1994), 2.2 ms (δ_2), and (3) EBURP-2 (Geen and Freeman 1991), 1.4 ms (δ_3). An *asterisk* indicates time and phase reversal of the corresponding pulse shape. The transfer delays are adjusted to $\tau_1 = 1/(4J_{NH}) - 0.5\,\delta_1 - 0.5\,\delta_2$, $\tau_2 = 1/(4J_{NH}) - 0.5\,\delta_1 - \kappa\delta_3$, and $\tau_3 = 1/(4J_{NH})$. These settings account for spin evolution during the various shaped ^{1}H pulses. The parameter $\kappa \approx 0.7$ can be fine tuned to equilibrate the transfer amplitudes of the different coherence transfer pathways for optimal suppression of the unwanted quadruplet components in the spectrum (Schulte-Herbrüggen and Sorensen 2000). Pulses are applied along the *x*-axis unless indicated. The phase ϕ_0 needs to be set to +y or −y, depending on the spectrometer, to add the signals originating from ^{1}H and ^{15}N polarization. Pulsed field gradients, G_1–G_8 are applied along the z-axis (PFG$_z$) with durations of 200 µs to 2 ms and field strengths ranging from 5 to 40 G/cm. The phase cycling is: $\phi_1 = -x,x$; $\phi_2 = -y$; $\phi_3 = -x$; $\phi_{acq} = -x,x$. The relative durations of G_5 and G_6 are given by the gyromagnetic ratios $G_5/G_6 = \gamma_H/\gamma_N$. For quadrature detection in t_1 (replacing the relaxation period Δ), echo-antiecho data are recorded by inverting the sign of gradient G_6 together with phases ϕ_2 and ϕ_3. **b** Numerical calculations of longitudinal spin-relaxation times T_1^H (*dotted black lines*), T_1^{Hsel} (*straight black lines*) and T_1^N (*dashed blue lines*) as a function of magnetic field and molecular tumbling correlation time. The computed ^{15}N relaxation-rate constants take into account dipolar ^{1}H-^{15}N and ^{15}N CSA interactions, assuming isotropic overall tumbling of the molecule described by a single rotational correlation time. ^{1}H longitudinal relaxation time constants were derived by numerical integration of the Solomon equations taking into account all ^{1}H-^{1}H dipolar interactions in the protein, and assuming different initial ^{1}H spin polarization for selective and non-selective excitation. More details on the simulation protocol used and the underlying assumptions can be found in a recent review by Schanda (2009). **c** Effect of the ^{15}N inversion pulse, applied after the signal detection period of the BEST-TROSY sequence, on the ^{15}N polarization recovery. The ^{15}N polarization is plotted as a function of the recycle delay (T_{rec}) without (*left panel*) and with (*right panel*) the additional ^{15}N pulse. The factor λ refers to the ^{15}N steady-state polarization enhancement as defined in (4)

sensitivity. This is realized in TROSY-type experiments (Pervushin et al. 1997, 1998; Brutscher et al. 1998) where single-transition states are detected, and both ^{1}H and heteronuclear spin polarization contribute to the NMR signal. TROSY spectroscopy, introduced more than 10 years ago, has been successfully applied to high-molecular weight perdeuterated proteins or nucleic acids. TROSY-type experiments are preferably performed at high magnetic field strength B_0 where line narrowing resulting from CSA-dipolar cross-correlation (Brutscher 2000) is most effective. Recent work on experimental determination of CSA tensors of amide moieties in polypeptides indicates that maximal TROSY line narrowing in the ^{15}N dimension is expected for ^{1}H Larmor frequencies in the 800 ± 200 MHz range (Yao et al. 2010a), while slightly higher field strengths, 1.2 ± 0.2 GHz are required for optimal TROSY effects in the ^{1}H dimension (Yao et al. 2010b). In the following, we will demonstrate that TROSY, when combined with BEST implementation also provides a sensitivity/resolution advantage for the study of moderately sized proteins without high-level deuteration.

Figure 1a shows the basic building blocks of a TROSY experiment: (1) an initial INEPT transfer block, (2) a relaxation period (Δ) as required for heteronuclear chemical shift editing or coherence transfer to other nuclei, (3) a single-transition to-single transition coherence transfer sequence (ST2-PT), and (4) a recycle delay (T_{rec}) including the detection period. In the following, we will focus on scalar-coupled ^{1}H-^{15}N spin pairs. The relevant coherence transfer pathways starting from ^{1}H and ^{15}N polarization are given as:

$$^1\text{H pathway: } H_z \xrightarrow{INEPT} \pm 2H_zN_x = \pm\left(H^{\alpha}N_x + \mathbf{H^{\beta}N_x}\right) \xrightarrow{ST2-PT} \pm \mathbf{N^{\beta}H_x} \quad (1)$$

$$^{15}\text{N pathway: } N_z \xrightarrow{INEPT} N_x = \left(H^{\alpha}N_x + \mathbf{H^{\beta}N_x}\right) \xrightarrow{ST2-PT} \mathbf{N^{\beta}H_x} \quad (2)$$

with the spin states selected by the ST2-PT sequence given in bold letters. Depending on the phase ϕ_0 of the last ^{1}H pulse in the INEPT sequence the two pathways either add or subtract, and the detected NMR signal will be proportional to the sum (or difference) of ^{1}H and ^{15}N

steady-state spin polarizations ($P_{tot}^{ss} = P_H^{ss} \pm P_N^{ss}$). So far, spin relaxation during the sequence has been neglected. Of course, spin relaxation will reduce the amount of signal detected for the two pathways, but it will also create a third additional coherence transfer pathway:

$$3\text{rd pathway} : \ldots \xrightarrow{\Delta} H_z \xrightarrow{ST2-PT} -N_z \xrightarrow{180^\circ_N} +N_z \qquad (3)$$

The ^{1}H spin polarization that builds up during the relaxation period Δ, and that corresponds to undetectable (lost) signal for the current scan, is transferred by the ST2-PT sequence into enhanced off-equilibrium ^{15}N polarization that will be available for the next scan as long as it survives relaxation during the recycle delay (T_{rec}). Note that an additional ^{15}N 180° pulse has been added to the TROSY sequence after the detection period in order to create ^{15}N polarization that is of the same sign as equilibrium polarization. This reduces polarization loss during T_{rec}, and thus further enhances the overall sensitivity of the experiment (Fig. 1c). After a few transients, a steady-state situation is established with ^{1}H and ^{15}N polarization depending on the relaxation rate constants T_1^H and T_1^N, and the relaxation delays Δ and T_{rec} as $P_H^{ss} = \langle H_z \rangle^{ss} \propto \gamma_H\left(1 - \exp\left(-T_{rec}/T_1^H\right)\right)$ and $P_N^{ss} = \langle N_z \rangle^{ss} \propto \gamma_N - \left(\left(\gamma_N - \gamma_H\left(1 - \exp\left(-\Delta/T_1^H\right)\right)\right)\right.$ $\left.\exp\left(-T_{rec}/T_1^N\right)\right)$.

In order for this third coherence transfer pathway (3) to contribute significantly to the detected signal, the buildup of ^{1}H polarization during the relaxation delay Δ needs to be efficient, while ^{15}N polarization decay during the recycle delay T_{rec} has to remain small. Therefore, in order to observe a significant effect, the ^{15}N longitudinal relaxation time must be significantly longer than that observed for ^{1}H, and the ^{1}H T_1 has to be comparable to the relaxation delay Δ. These conditions are generally not fulfilled for amide ^{1}H-^{15}N spin pairs in moderately sized proteins using standard (hard-pulse based) TROSY sequences at the currently available magnetic field strengths (Fig. 1b). The situation, however, changes dramatically in BEST-type experiments where the relation $T_1^{Hsel} \ll T_1^N$ is satisfied even at moderate magnetic field strengths. The short T_1^{Hsel} of a few hundred milliseconds allows for fast repetition rates (50 ms $< T_{rec} <$ 500 ms) while retaining optimal sensitivity. To get a quantitative estimate of the enhancement effect achieved by the additional coherence transfer pathway, we define an enhancement factor λ of the steady-state

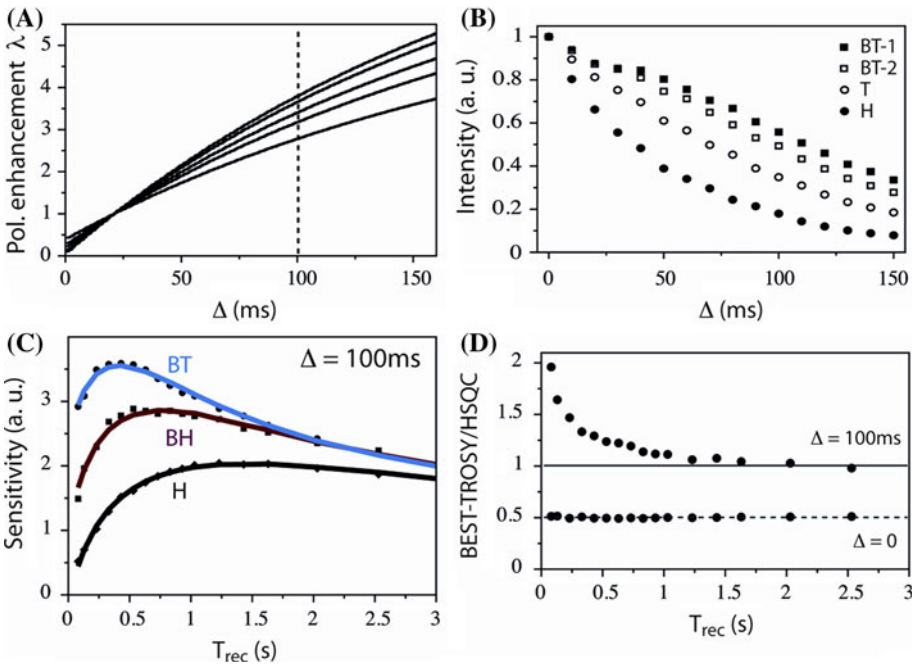

Fig. 2 Simulated (**a**) and experimental (**b**–**d**) data for ubiquitin at 5°C and 800 MHz (estimated $T_1^{Hsel} = 200$ ms and $T_1^N = 1$ s). Experimental data points are obtained from integration of 1D spectral intensities over the amide ^{1}H region (8.5–10 ppm). **a** Enhancement factor λ (4) computed as a function of the relaxation delay Δ. The different curves correspond (from *top* to *bottom*) to recycle delays of $T_{rec} = 50$, 100, 200, 300, and 500 ms, respectively. **b** Apparent signal decay when incrementing the relaxation delay Δ in HSQC (**H**), TROSY (**T**), BEST-TROSY with $T_{rec} = 100$ ms (**BT-1**), and BEST-TROSY with $T_{rec} = 200$ ms (**BT-2**). **c** Sensitivity curves for HSQC (**H**), BEST-HSQC (**BH**) and BEST-TROSY (**BT**) measured for Δ = 100 ms. **d** Sensitivity gain of BEST-TROSY versus BEST-HSQC as a function of the recycle delay for Δ = 0 and Δ = 100 ms

^{15}N polarization with respect to its thermal equilibrium value as:

$$\lambda = P_N^{ss} \Big/ P_N^{eq} = 1 - \left(\left(1 - \gamma_H/\gamma_N\left(1 - \exp\left(-\Delta/T_1^H\right)\right)\right)\exp\left(-T_{rec}/T_1^N\right)\right) \quad (4)$$

In the following we will focus on the small model protein ubiquitin (8.6 kDa). At 5°C this protein has a tumbling correlation time of ~8 ns. The polarization enhancement calculated from (4) is plotted in Fig. 2a as a function of the relaxation delay Δ for different recycle delays T_{rec}. ^{15}N polarization enhancement ranging from a factor of two up to a factor of four is expected for a relaxation delay, Δ, of 100 ms using short recycle delays. Figure 2b–d show experimental data for ubiquitin that illustrate how this polarization enhancement translates into reduced apparent spin relaxation during the delay Δ (Fig. 2b), and thus to a significant sensitivity (constant delay Δ) or resolution (incremented delay $\Delta = t_1$) gain of BEST-TROSY with respect to BEST-HSQC (Fig. 2c). Without relaxation delay ($\Delta = 0$, $t_1 = 0$) the third coherence transfer pathway (3) does not contribute to the detected signal, and therefore the HSQC version yields, as expected, twice the signal of the TROSY version (Pervushin et al. 1997). The situation is inverted when longer relaxation (Δ or t_1) delays are used (Fig. 2d). For $\Delta = 100$ ms, the TROSY ^{15}N line narrowing results in a doubling of peak intensity (data at long T_{rec} values), while an additional signal gain (up to 100%) is observed for short recycle delays due to the ^{15}N polarization enhancement effect described above. Figure 3 shows a comparison of BEST-HSQC and BEST-TROSY implementations in HNCO and iHNCA correlation experiments (Lescop et al. 2007) where the two ^{15}N-^{13}C transfer periods play the role of the relaxation delay, Δ, required for the ^{15}N polarization enhancement. Significantly higher signal intensity is obtained for BEST-TROSY (when compared to BEST-HSQC) with S/N gains ranging from a factor of 1.2 to 2.8 (average of 1.7) for the HNCO, and from 1.3 to 3.5 (average of 2.1) for the iHNCA experiment. If we compare BEST-TROSY with a standard, hard-pulse based

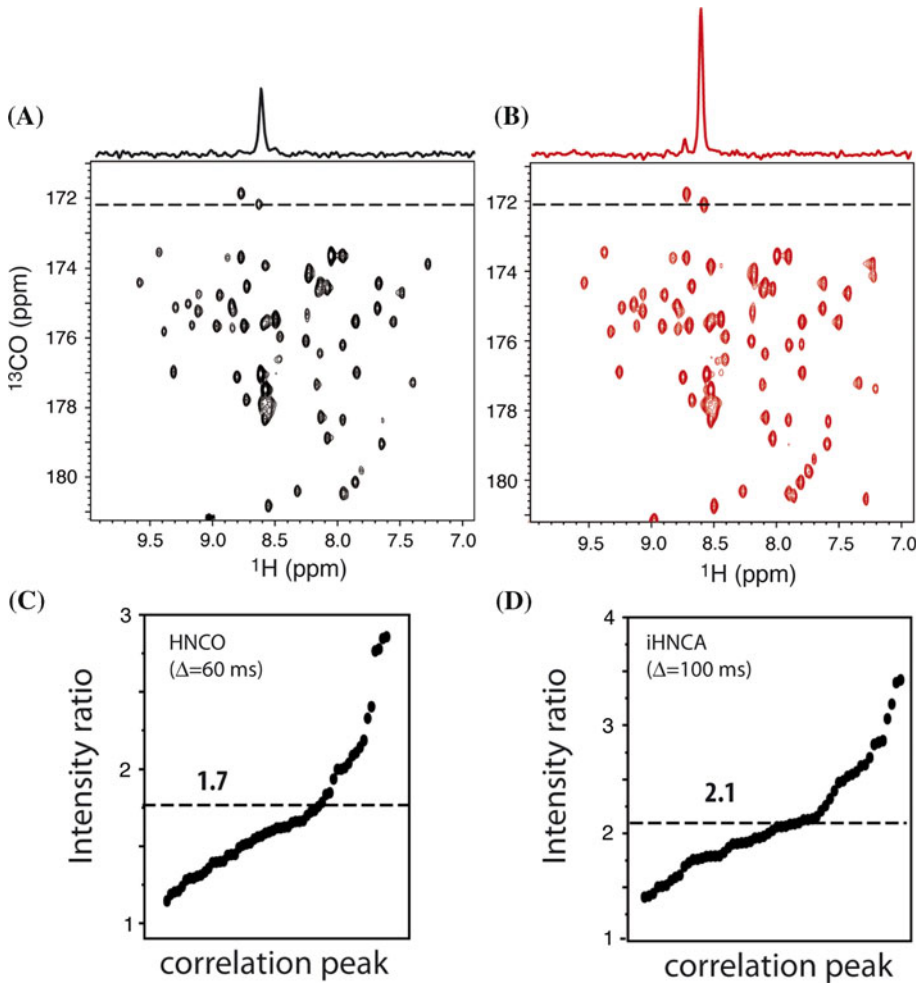

Fig. 3 2D H(N)CO correlation spectra of ubiquitin (5°C, 800 MHz, $T_{rec} = 250$ ms) using either BEST-HSQC (**a**) or BEST-TROSY (**b**) implementations. The peak intensity ratio measured for each correlation peak is plotted in **c** for HNCO, and in **d** for iHNCA. The *dashed line* and associated value indicate the average intensity gain achieved by BEST-TROSY

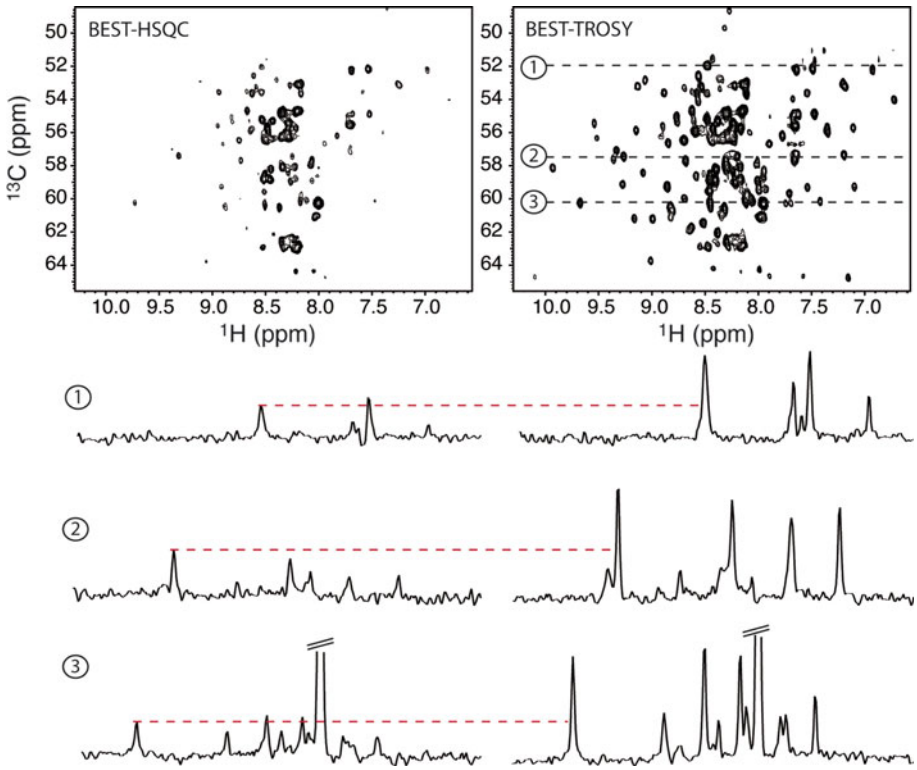

Fig. 4 2D ^{1}H-^{13}C iHNCA correlation spectra of a 138-residue (16 kDa) bacterial protein currently studied in our laboratory. Data sets were recorded at a sample temperature of 20°C on an 800 MHz spectrometer. At this temperature, the protein has a tumbling correlation time of $\tau_c \approx 10$ ns as estimated from 1D ^{15}N relaxation measurements. The results achieved with either BEST-HSQC or BEST-TROSY implementations in the same total experimental time are shown in the *left* and *right* panels, respectively. In addition, three characteristic 1D ^{1}H traces extracted from the 2D planes are shown to highlight the sensitivity gain achieved by BEST-TROSY

experiment, the overall sensitivity gain is even more impressive, as an additional S/N gain of a factor of 1.5–2.0 is achieved for high repetition rates by the BEST implementation that adds to the BEST-TROSY signal enhancement discussed above. As a second example, we have recorded iHNCA spectra for a 16 kDa protein. At 20°C, this protein has an estimated tumbling correlation time of $\sim$10 ns, and therefore the ratio of ^{15}N and ^{1}H T_1 relaxation rates (see Fig. 1b) is supposed to be even more favorable for relaxation-induced ^{15}N polarisation enhancement. This is confirmed by the experimental data (Fig. 4) which show that a slightly higher intensity gain is achieved by the BEST-TROSY version than what has been observed for ubiquitin.

Another important protein application that will strongly benefit from the ^{15}N-polarization enhancement feature of BEST-TROSY is the long-range HNCO experiment which is used for the detection of trans-hydrogen-bond $^{2h}J_{NC'}$ scalar couplings (Cordier and Grzesiek 1999). In this experiment, the ^{15}N-^{13}C transfer time has to be set to $n/^{1}J_{NC'} \approx n \times 66.7$ ms (with $n = 1$ or 2) for efficient coherence transfer via the small couplings $^{2h}J_{NC'} < 0.9$ Hz. Because of the resulting long ^{15}N relaxation delays (for $n = 1$ $\Delta = 133.3$ ms), the sensitivity drops quickly for slower tumbling molecules, and thus high-level deuteration is generally required to make this experiment successful. Figure 5 shows a comparison of long-range HNCO data

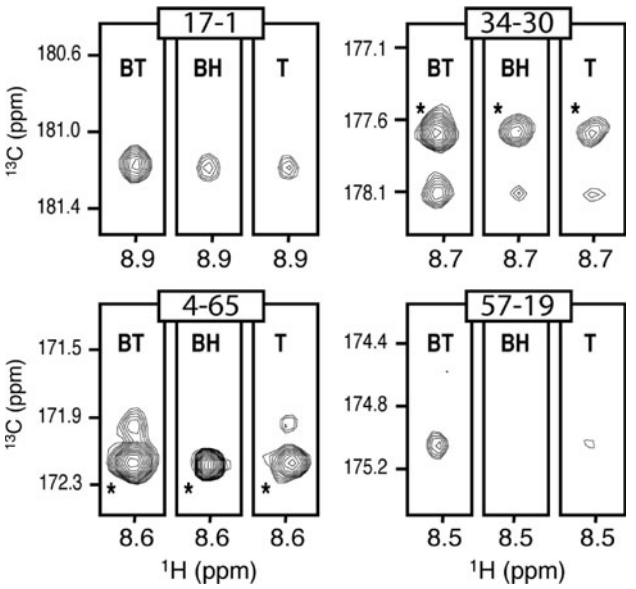

Fig. 5 Long-range 3D HNCO correlation spectra of ubiquitin (2 mM, pH 7.2, 5°C, 800 MHz, $\Delta = 133.3$ ms) recorded with a BEST-TROSY (**BT**), BEST-HSQC (**BH**), and standard TROSY (**T**) implementation. The recycle times were set to $T_{rec} = 270$ ms for BEST (**BT** and **BH**), and $T_{rec} = 1$ s for hard-pulse (**T**) experiments. The total experimental time was 17 h per 3D spectrum. 2D ^{1}H-^{13}C spectral regions for 4 representative H-bond correlations are shown: 17 (N)–1 (CO) in β-sheet (J = 0.53 Hz); 34 (N)–30 (CO) in α-helix (J = 0.64 Hz); 4 (N)–65 (CO) in β-sheet (J = 0.60 Hz); 57 (N)–19 (CO) in an irregular structural element (J = 0.39 Hz). A *star* indicates a residual sequential correlation peak

recorded for fully protonated ubiquitin at 5°C using either a standard hard-pulse based water-flip-back TROSY, a BEST-HSQC, or a BEST-TROSY sequence. Each 3D data set has been recorded in an experimental time of 17 h. Only the BEST-TROSY version yields sufficient sensitivity to detect a large number (24) of trans-hydrogen-bond correlation peaks. The S/N ratio in the two other data sets is a factor of 2–3 lower, making many trans-hydrogen-bond correlations difficult or impossible to detect. Based on the reported $^{2h}J_{NC'}$ coupling constants for ubiquitin (Cordier and Grzesiek 1999), we can estimate the detection limit in the BEST-TROSY data set, recorded on a fully protonated protein sample, to be $^{2h}J_{NC'} > 0.35$ Hz.

In summary, we have introduced an efficient polarization enhancement mechanism as a built-in feature of BEST-TROSY-type NMR pulse sequences. This feature is conceptually similar to the ISIS technique (Riek 2001), introduced a few years ago to enhance steady-state magnetization in conventional TROSY experiments by applying an additional ST2-PT (or refocused INEPT) sequence during the recycle delay T_{rec}. For ISIS, signal enhancements of 10–25% have been observed for individual amide groups in large deuterated proteins (Riek 2001). We have performed a theoretical evaluation of the performance of ISIS for different implementations and T_1^N/T_1^H ratios that can be found in the Supporting Information available for this article. These calculations show that a sensitivity enhancement of 25% is close to the theoretical maximum achievable by the ISIS technique, and that it requires T_1^N/T_1^H ratios larger than five. We have shown here that BEST-TROSY can yield much higher S/N improvements (of more than a factor of two) for proteins with a high protonation level, without the need of any pulse sequence modification or parameter optimization. The ^{15}N polarization enhancement will be most pronounced for experimental applications that require long ^{15}N transverse relaxation delays. Moreover, BEST-TROSY allows for short overall experimental times, or long maximal evolution times (for high spectral resolution) in all dimensions without the need for unconventional data sampling methods. Therefore, this technique will be beneficial for NMR investigations of moderately sized proteins that do not require high-level deuteration, as well as for RNA and DNA studies (Farjon et al. 2009). Further sensitivity improvements are expected when using even higher field magnets as the ^{15}N T_1 increases with B_0 while the selective ^1H T_1 is field independent (see Fig. 1b), a situation that favors the ^{15}N polarization enhancement effect described here. Therefore, at the highest magnetic field strengths currently available (800–1,000 MHz), BEST-TROSY implementations will yield highest sensitivity, compared to BEST-HSQC or standard hard-pulse-based versions, for most H–N–C correlation experiments that are required for sequential resonance assignment or spin coupling measurements in proteins and nucleic acids.

Acknowledgments We thank Drs J. Boisbouvier, S. Hediger, and M. Plevin for stimulating discussion and critical reading of this manuscript, and I. Ayala for expert protein production. This work was supported by the Commissariat à l'Energie Atomique, the Centre National de la Recherche Scientifique, the University of Grenoble, and the French research agency (grant ANR 08-BLAN-210) and the European Commission (FP7-I3 BIO-NMR contract No. 261863).

References

Brutscher B (2000) Principles and applications of cross-correlated relaxation in biomolecules. Concepts Magn Reson 12(4): 207–229

Brutscher B, Boisbouvier J, Pardi A, Marion D, Simorre JP (1998) Improved sensitivity and resolution in H-1-C-13 NMR experiments of RNA. J Am Chem Soc 120(46):11845–11851

Cordier F, Grzesiek S (1999) Direct observation of hydrogen bonds in proteins by interresidue (3 h)J(NC′) scalar couplings. J Am Chem Soc 121(7):1601–1602

Farjon J, Boisbouvier J, Schanda P, Pardi A, Simorre JP, Brutscher B (2009) Longitudinal relaxation enhanced NMR experiments for the study of nucleic acids in solution. J Am Chem Soc 131:8571–8577

Geen H, Freeman R (1991) Band-selective radiofrequency pulses. J Magn Reson 93:93–141

Kupce E, Freeman R (1994) Wide-band excitation with polychromatic pulses. J Magn Reson A 108(2):268–273

Lescop E, Schanda P, Brutscher B (2007) A set of BEST triple-resonance experiments for time-optimized protein resonance assignment. J Magn Reson 187(1):163–169

Lescop E, Kern T, Brutscher B (2010) Guidelines for the use of band-selective radiofrequency pulses in hetero-nuclear NMR: example of longitudinal-relaxation-enhanced BEST-type H-1-N-15 correlation experiments. J Magn Reson 203(1):190–198

Pervushin K, Riek R, Wider G, Wüthrich K (1997) Attenuated T-2 relaxation by mutual cancellation of dipole-dipole coupling and chemical shift anisotropy indicates an avenue to NMR structures of very large biological macromolecules in solution. Proc Natl Acad Sci USA 94(23):12366–12371

Pervushin K, Riek R, Wider G, Wüthrich K (1998) Transverse relaxation-optimized spectroscopy (TROSY) for NMR studies of aromatic spin systems in C-13-labeled proteins. J Am Chem Soc 120(25):6394–6400

Pervushin K, Vögeli B, Eletsky A (2002) Longitudinal H-1 relaxation optimization in TROSY NMR spectroscopy. J Am Chem Soc 124(43):12898–12902

Riek R (2001) Enhancement of the steady-state magnetization in TROSY experiments. J Biomol NMR 21(2):99–105

Schanda P (2009) Fast-pulsing longitudinal relaxation optimized techniques: enriching the toolbox of fast biomolecular NMR spectroscopy. Prog NMR Spectrosc 55(3):238–265

Schanda P, Brutscher B (2005) Very fast two-dimensional NMR spectroscopy for real-time investigation of dynamic events in proteins on the time scale of seconds. J Am Chem Soc 127(22):8014–8015

Schanda P, Kupce E, Brutscher B (2005) SOFAST-HMQC experiments for recording two-dimensional heteronuclear correlation spectra of proteins within a few seconds. J Biomol NMR 33(4):199–211

Schanda P, Van Melckebeke H, Brutscher B (2006) Speeding up three-dimensional protein NMR experiments to a few minutes. J Am Chem Soc 128(28):9042–9043

Schulte-Herbrüggen T, Sorensen OW (2000) Clean TROSY: compensation for relaxation-induced artifacts. J Magn Reson 144(1):123–128

Yao LS, Grishaev A, Cornilescu G, Bax A (2010a) Site-specific backbone amide N-15 chemical shift anisotropy tensors in a small protein from liquid crystal and cross-correlated relaxation measurements. J Am Chem Soc 132(12):4295–4309

Yao LS, Grishaev A, Cornilescu G, Bax A (2010b) The impact of hydrogen bonding on amide H-1 chemical shift anisotropy studied by cross-correlated relaxation and liquid crystal NMR spectroscopy. J Am Chem Soc 132(31):10866–10875